JOURNAL OF APPLIED ELECTROCHEMISTRY 12 (1982) 127–133

Oxide anodes in electro-organic oxidation. Oxidation of maleic acid on tungsten oxide anodes

G. FILARDO, F. DI QUARTO, S. GAMBINO, G. SILVESTRI

Istituto di Ingegneria Chimica, Facoltà di Ingegneria, Università di Palermo, Viale delle Scienze, Palermo, Italy

Received 18 March 1981

The electrochemical oxidation of maleic acid on tungsten anodes has been investigated. Glyoxal and carbon dioxide were the main products together with tartaric acid and acetaldehyde. Glyoxal is also obtained as the main product from the oxidation of *d*-tartaric acid. Under the same conditions succinic acid is completely oxidized to carbon dioxide and water. The anodic dissolution of tungsten and the oxidation of water to oxygen become predominant in the final stages of the electrolyses.

1. Introduction

Although the electrochemical oxidation of organic compounds has been widely studied, only a limited number of electrode materials have been tested so far, i.e. platinum, graphite, lead and to a lesser extent, nickel, DSA, gold and silver. As the anodic surface may play a prominent role in directing the reaction towards specific products, an investigation of the catalytic properties of other kinds of electrode materials appears necessary.

In this paper, the first results of some research dealing with the use of some valve metal anodes in the oxidation of unsaturated compounds are reported. The large potential drop due to the electric behaviour of these anodes makes them less attractive for use in synthetic processes [1]. In fact, this research was stimulated by the results of an earlier study in this laboratory on the electrochemical formation of tungsten oxides by anodization of tungsten in different acidic media [2–5]. In the course of these studies it was observed that these anodes can be used at temperatures $\geqslant 70^\circ$ C, at reasonable current densities (2–8 mA cm^{-2}) and cell voltages (18–22 V in diaphragmless cells). Therefore, we have examined the oxidation of some unsaturated organic compounds under the same conditions.

The results reported here are related to the oxidation of maleic acid. Several authors have reported that different products are obtained from the anodic oxidation of this acid, depending on the anodic materials employed in the process e.g. acetylene [6], oxalic and formic acids and acetaldehyde [7] at platinum in alkaline media, and formic and tartaric acids at PbO_2 in aqueous sulphuric acid [8].

2. Experimental procedure

Pure reagents (Fluka, Carlo Erba) and distilled water were used. All the electrolyses were carried out in H-shaped cells (internal volume 100 cm^3) with a grade 4 glass frit diaphragm. Both compartments were magnetically stirred. The anolyte was 0.1 N H_2SO_4 with 0.1–1 N organic acid. The catholyte was 1 N H_2SO_4. All the electrolyses were performed at 70 ± 0.2° C. Tungsten electrodes were made of spectrographically pure metal sheets 0.1 mm thick with a surface area of 25 cm^2. The electrodes were electropolished in 15% NaOH at room temperature, rinsed with distilled water and dried in a stream of nitrogen.

Voltage–time measurements were performed with current densities in the range 2–8 mA cm^{-2} using an AMEL 552 Potentiostat-Galvanostat. The cell voltage was measured by a multimeter Simpson 360 and was continuously recorded. Before the electrolyses was carried out the system was flushed for some time with 99.9% helium.

0021–891X/82/010127–07$02.70/0

Gases formed during the electrolyses in the anodic and cathodic compartments of the cell were collected separately and measured in two gas meters. The compositions of the gases were determined by periodical glc analyses (HP, 620 gas chromatograph equipped with a TC detector and a Porapak Q column, 60° C, 25 cm^3 min^{-1} He).

At the end of each electrolysis both anolyte and catholyte were tested with 2,4-dinitrophenylhydrazine solutions. Carbonyl compounds were found in the anolyte, but never in the catholyte. A fraction of the anolyte was usually reacted with 2,4-dinitrophenylhydrazine to separate the carbonyl compounds. Qualitative analyses of the mixtures of 2,4-dinitrophenylhydrazones were performed by thin layer chromatography on neutral alumina with a 2:1 mixture of cyclohexane–nitrobenzene as the developing solvent.

Acetaldehyde was revealed in traces both in the anodic gases and in the anolyte. Apart from traces of other unidentified carbonyl products, the glyoxal bis-2,4-dinitrophenylhydrazone was the predominant carbonyl compound in the anolyte. Glyoxal bis-2,4-dinitrophenylhydrazone was identified by melting point measurements, infrared and mass spectroscopy.

Samples of the anolyte from the experiments with maleic acid were neutralized with NaOH, dried under vacuum and extracted with methanol. The methanolic solution, at − 50° C, was treated with diazomethane and examined by gas chromatography. As well as the dimethylester of the unreacted maleic acid being present, racemic and *meso*-dimethyltartrate and heavier unidentified products were present.

Among the anodic reactions tungsten dissolution and formation of $WO_3 \cdot H_2O$ layers also occurs: the yield of this process was calculated on the basis of weight loss from the anode after each experiment. No changes in morphology of the hydrated oxide layers was caused by the organic acid. This comparison was made by means of direct X-ray diffraction patterns of the anodic films, using a Philips Model PW 1130 generator and a PW 1050 goniometer. CuKα radiation was used at a scanning rate of $2\theta = 1°\,min^{-1}$. The *d*-spacings were measured and compared with the ASTM index values. The data reported by Glemser *et al.* [9, 10] were used for the identification of the hydrated oxides.

3. Results

3.1. *Blank experiments*

The dependence of the anodic behaviour of tungsten in acidic solutions on the temperature and electrolyte compositions has been already described [2–5] but will be summarized here briefly to allow a better comparison with the experimental data obtained when organic species are present in the anolyte. The voltage–time curves at constant current densities of 2–8 mA cm^{-2}, obtained with cells such as

$$\text{(anode) W/H}_2\text{SO}_4\text{(0.05–6 N)/Pt (cathode)} \quad (1)$$
$$t = 70° \text{ C}$$

have the shape shown in Fig. 1, curve a, for which two stages are recognizable. In the first stage there is a sharp increase in the voltage due to the formation of an amorphous barrier film on the anode, according to the reaction:

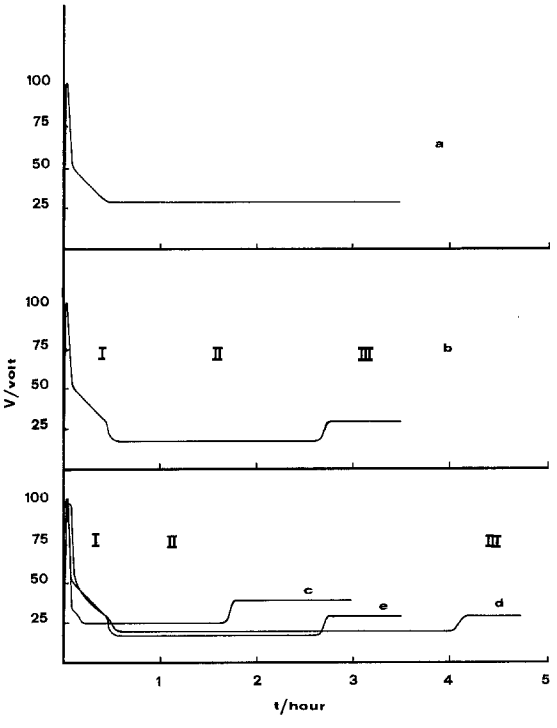

Fig. 1. Voltage–time curves recorded at 70° C and i = 8 mA cm^{-2} at different solutions: (a) 0.1 N H_2SO_4, (b) 0.1 N H_2SO_4 + 1 N maleic acid, (c) 0.1 N H_2SO_4 + 1 N *d*-tartaric acid (i = 14 mA cm^{-2}), (d) 0.1 N H_2SO_4 + 1 N succinic acid and (e) 0.1 N H_2SO_4 + 0.4 N fumaric acid.

$$W + 3H_2O \rightarrow WO_3 + 6H^+ + 6e^- \quad (2)$$

After the maximum voltage is reached vigorous oxygen evolution is observed and a localized corrosion process leads to the formation of a yellow-green crystalline porous oxide layer on the underlying amorphous barrier film.

The second stage corresponds to the attainment of a steady electrode potential, with continued growth of the porous layer of crystalline $WO_3 \cdot H_2O$ with oxygen evolution as the main anodic reaction. The corrosion reaction accounts for not more than 3% of the charge. Layers with good mechanical stability are obtained using the above conditions.

3.2. *Experiments with maleic acid*

When maleic acid is added to Cell 1, the voltage–time curve is significantly modified and the processes taking place at the anode are different to those mentioned above.

Fig. 1b shows the voltage–time curve of a typical experiment in which the anolyte is 1 N maleic acid and 0.1 N sulphuric acid at 70° C and 8 mA cm^{-2}. It is possible to define three stages of this curve:

Stage I, during which there is a rapid variation of the voltage which is analogous to curve a.

Stage II, during which the voltage is constant at a value of about 16–17 V. The quantity of charge passed during this stage depends on various parameters such as the maleic acid concentration, the anodic current density and the stirring of the solution.

Stage III, during which the cell reaches a steady voltage at the same value observed in curve a.

The oxidation of maleic acid occurs essentially during stage II and hence experiments were designed to define the electrochemical and chemical phenomena taking place during this stage.

3.2.1. *Electrochemical phenomena.* As already stated, in the range of conditions discussed so far (0.1–2 N maleic acid, 2–8 mA cm^{-2} current density) the voltage of stage II is fairly independent of the anodic current density and the concentrations of maleic and sulphuric acids, and remains quite constant between 16 and 17 V. It can be seen from the data in Table 1 that the charge passed during stage II varies with the initial concentration of maleic acid. An increase in the charge passed was also observed when, at constant maleic acid concentration, increasing currents were imposed during galvanostatic experiments. At the same time there was a decrease in the duration of this stage (see Fig. 2). Stirring of the anolyte has also been observed to influence the duration of this stage; in unstirred solutions stage II was 20% shorter than when the solution was stirred.

Table 1. Dependence of the charge passed during stage II on the initial concentration of maleic acid

Maleic acid concentration (N)	*Charge* (C)
0.05	970
0.1	1190
0.25	1400
0.5	1510
1.0	1590

The experiment was performed at 70° C and 8 mA cm^{-2} with 0.1 N sulphuric acid and 1 N maleic acid in the anolyte.

Finally, it is worth noting the results obtained in some experiments in which maleic acid, absent at the beginning, was added after the passage of different quantities of electrical charge. If the addition of the maleic acid is made when the porous layer is sufficiently thin (within or just after the end of stage I) the system behaves in the

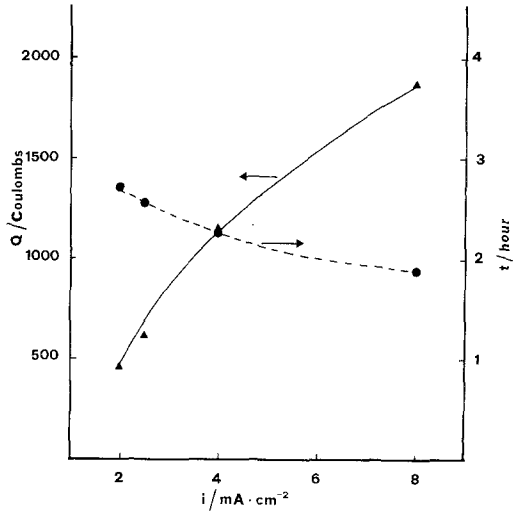

Fig. 2. Influence of current density on the charge and on the duration of stage II. The composition of the anolyte was: 0.1 N H_2SO_4 and 1 N maleic acid.

same way as when the organic acid is present from the beginning of the experiment (see curve b in Fig. 1). If the addition is made when a very thick porous layer is present, no changes in the anodic charging curve with respect to Fig. 1a takes place and only 3% of the circulated charge is used in the oxidation of maleic acid.

In experiments in undivided cells, a stable coating of a mixture of reduced oxides on the cathode surface is obtained. The same kind of coating is also obtained when lengthy experiments in diaphragm cells were performed. Since the amount of the oxide deposited is independent of the current density, but proportional to the quantity of charge passed, it seems likely that the layer is formed by electrophoretic deposition of colloidal particles on the cathode surface.

3.2.2. *Electro-organic processes.* The oxidation of maleic acid takes place predominantly during stage II. This is confirmed by the data in Table 2, in which the gases evolved at the anode and the anodic losses are correlated to the quantity of charge passed through the cell.

During stage I the most important reactions are the WO_3 formation (according to Reaction 2) and oxygen evolution. Thus, the coulometric balance is in good agreement with these reactions, which contribute 13 and 81% of the total charge.

During stage II maleic acid is clearly involved, as large amounts of carbon dioxide arise from the anode. The mean gas compositions are: 36% O_2 and 64% CO_2. In addition to oxygen evolution and formation of WO_3 (21 and 11%, respectively of the charge), the oxidation of maleic acid to glyoxal and CO_2 occurs following the overall stoichiometry:

$$C_4H_4O_4 + 2H_2O \rightarrow C_2H_2O_2 + 2CO_2 + 6H^+ + 6e^- \quad (3)$$

The quantity of glyoxal obtained corresponds to a molar ratio of $C_2H_2O_2/CO_2$ of about 0.5. Apart from traces of acetaldehyde no other C_2 or C_3 carbonyl derivatives were found. The CO_2 evolved, according to Reaction 2 accounts for 20% of the circulated charge. The data of Table 2 show clearly that maleic acid is oxidized only to a limited extent during stage II. The end of this stage is therefore not due to significant variations in the concentrations of the acid, and so must be caused by other factors. In fact, it has been observed that cleaning the electrode as soon as stage III begins allows the recording of the same charging curves with the sequence of stages I, II and III several times in the same solution.

3.3. *Experiments with fumaric, tartaric, succinic and acetic acids*

A comparison between the behaviour of maleic acid and other C_4 dicarboxylic acids allows some conclusions to be drawn about the sequence of reactions leading from maleic acid to glyoxal and carbon dioxide.

As in the case of maleic acid electrochemical and chemical phenomena are separately outlined in the following.

3.3.1. *Electrochemical phenomena.* Fig. 1 (curves c, d and e) shows the voltage–time curves for the oxidation of *d*-tartaric, succinic and fumaric acids, under the same conditions used for maleic acid. The curves show a sequence of three stages analogous to those recorded for maleic acid. The differences observed between these systems are related to tungsten corrosion and the length of stage II. The results of some experiments using 0.4 N fumaric acid (corresponding to the saturation concentration at 70° C), 1 N succinic acid and 1 N tar-

Table 2. Maleic acid oxidation. Distribution of the charge between the competing anodic reactions

Stage	*Total charge* (C)	*Oxygen evolution* (C)	*Carbon dioxide evolution* (C)	*Tungsten losses as* W^{6+} (C)
I	360	290	13	47
II	1590	330	312	180
III	590	495	67	13

The experiment was performed at 70° C and 8 mA cm^{-2} with 0.1 N sulphuric acid and 1 N maleic acid in the anolyte.

Table 3. Influence of the nature of the acid on the corrosion processes

Acid	*Current density* ($mA\ cm^{-2}$)	*Percentage of charge used in anodic corrosion*	
		Stage II	*Stage III*
Maleic acid	8	11.3	2.3
Fumaric acid	8	13	3
Succinic acid	8	5	3
d-Tartaric acid	14	66	23

Maleic, succinic and *d*-tartaric acid concentrations of 1 N were used with 0.1 N H_2SO_4.
A fumaric acid concentration of 0.4 N, corresponding to saturation in 0.1 N H_2SO_4 at 70° C was used.

taric acid, at $8\ mA\ cm^{-2}$ and 70° C, are summarized in Table 3.

Fumaric acid (Fig. 1, curve e) does not show significant differences from maleic acid. Succinic acid clearly depresses the corrosion process during stage II, which is significatively longer for succinic acid than for the other acids (see Fig. 1, curve d). On the contrary, in the presence of *d*-tartaric acid, the anodic dissolution of tungsten is the only process taking place at a current of $8\ mA\ cm^{-2}$. Increasing the current to $14\ mA\ cm^{-2}$, the voltage–time curve of Fig. 1c is obtained. In this case 66% of the charge is consumed by corrosion during stage II, and the 23% during stage III.

3.3.2. *Electro-organic processes.* The same stoichiometry as maleic acid is observed when fumaric acid is employed. In the case of tartaric acid at higher anodic currents, organic oxidation is obtained and a decarboxylation process giving almost exclusively carbon dioxide and glyoxal is observed. In stage II the coulometric balance related to the oxidation is close to 90% when the following stoichiometry is considered:

$$C_4H_6O_6 \rightarrow C_2H_2O_2 + 2CO_2 + 4H^+ + 4e^-. \qquad (4)$$

A different picture is observed for succinic acid. Here the two most important anodic processes are oxygen production and complete oxidation of succinic acid to CO_2. No significant amounts of partial oxidation products were found in the anolyte, and the amount of CO_2 evolved and the coulometric balance are consistent with the stoichiometry:

$$C_4H_6O_4 + 4H_2O \rightarrow 4CO_2 + 14H^+ + 14e^-. \qquad (5)$$

Once stage III is reached, no significant differences in the behaviour of systems containing maleic, fumaric or succinic acids and systems containing sulphuric acid alone are noticeable (compare stage III of curves b, c and e in Fig. 1 with stage II of curve a). In fact, in the final stage, the main reaction is oxygen evolution, which consumes about 90% of the charge, while organic acid oxidation and anodic corrosion of tungsten each use about 3% of the charge.

The figures for *d*-tartaric acid are quite different, being about 70% for oxygen evolution, 3% for organic oxidation and 23% for anodic corrosion of tungsten.

Acetic acid was also tested in order to obtain more information about the reaction mechanism. In this case methyl acetate was the only product of the oxidation, leading to the deduction that the anodic decarboxylation goes through the cationic mechanism already described for the process known as the Hofer–Moest reaction:

$$-\overset{|}{\underset{|}{C}}-COO^- \rightarrow CO_2 + -\overset{|}{\underset{|}{C^+}} + 2e^-. \qquad (6)$$

4. Discussion

The following conclusions may be drawn.

(1) The tungsten anode behaves in the same way in organic acid solutions as in H_2SO_4 alone, except during stage II, when a limited oxidation of the organic acid takes place.

(2) When a strong chelating agent such as tartaric acid is present the corrosion process plays a more important part in the anodic reactions.

The relatively low voltage of stage II can be explained by looking at the structure of the oxide layers at the anode. In fact, the amorphous barrier film is responsible for the voltage drop, and has a

practically constant thickness during stage II, as demonstrated by the constant voltage maintained by the system under amperostatic conditions. During this stage, the corrosion process, represented by Reaction 2, consumes a fraction of the charge more significant than in the following stage III. This behaviour is consistent with the fact that tartaric acids have been found as intermediates in maleic acid oxidation to glyoxal, and that, in the experiments with tartaric acid, the corrosion process is the predominant anodic reaction.

At the end of stage II the amorphous layer undergoes a substantial increase in thickness to that found in stage III.

The growth of the crystalline porous layer in our system is analogous to that seen with H_2SO_4 alone and one could conclude that the growth of this layer starts at the beginning of stage II. This occurs at the expense of anodic dissolution and continues at a rate which depends on the fraction of the overall current which is involved in corrosion. The thickening of the porous layer extends into the region between the bulk of the solution and the underlying electrode surface, in which the mass transfer of the organic species is driven mainly by diffusive transport. The experimental data obtained for the parameters influencing the length of stage II are consistent with the view that the end of this stage is not due to a decisive variation of the composition of the bulk of the solution, but to the limiting conditions of mass transfer of the organic species through the porous layer.

In connection with this it is worth noting the following observations which are consistent with this interpretation:

The length of stage II is inversely proportional to the corrosion rate observed for the various acids.

The stirring of the solution has a direct influence on the length of stage II.

The voltage and the shape of the charging curve during stage II do not depend on the nature of the electro-organic process taking place at the anode: no differences, except for the length of the stage, were found between maleic and fumaric acids, which are oxidized to glyoxal, and succinic acid, whose oxidation is not selective and gives rise only to water and carbon dioxide.

No significant differences were observed in the behaviour of the systems containing different acids once stage III was reached.

On cleaning the anode once stage III had started and using it again in the same solution, it was possible to observe stages I, II and III again several times.

The addition of an organic species to the anolyte composed of aqueous sulphuric acid alone, when the porous layer was thick enough, did not modify the anodic processes: the shape of the charging curve was not affected and no significant quantities of the organic species were oxidized.

In the chemical process leading to glyoxal formation from maleic or fumaric acids, tartaric acid was found in the anolyte and the oxidation of the double bond probably preceeds decarboxylation. The reaction sequence proposed is

$$\mathrm{HOOC{-}CH{=}CH{-}COOH + 2H_2O} \rightarrow \mathrm{HOOC{-}CHOH{-}CHOH{-}COOH + 2H^+ + 2H_2O} \quad (7)$$

$$\mathrm{HOOC{-}CHOH{-}CHOH{-}COOH + 2H_2O} \rightarrow \mathrm{(HO)_2CH{-}CH(OH)_2 + 2CO_2 + 4e^- + 4H^+} \quad (8)$$

and this is consistent with a value of about 0.5 for the glyoxal to carbon dioxide molar ratio and with the results of tartaric acid oxidation where glyoxal and carbon dioxide were again obtained.

The last reaction has already been quoted in the literature: glyoxal was reported among several other products of the anodic oxidation of tartaric acid in aqueous solution [11].

The following comments about the mechanism of Reactions 7 and 8 may be made:

Reaction 7: both *meso* and *d,l*-tartaric acid were identified in the anolyte. Therefore the oxidation proceeds through some intermediate where rotation of the bond between carbons 2 and 3 must be free.

Reaction 8: as seen with acetic acid, in our system, decarboxylation follows a cationic mechanism which should lead to a structure like $-CH{=}CH^+$. From such an intermediate it is reasonable to suppose the formation of glycolic compounds such as an aldehyde or acid. The cationic intermediate arising from the decarboxylation of tartaric acid is, however, the obvious precursor of glyoxal: $-CH(OH)^+ + H_2O \rightarrow -CH(OH)_2 + H^+$.

The most disappointing feature of the results is their inability to realize a quantitative conversion of the organic species during stage II. Only the use of wiper blades [12] or other cleaning equipment adapted to remove the crystalline oxide layer would allow long-term preparative electrolyses with these anodes.

Acknowledgement

This research was supported by the Italian Consiglio Nazionale delle Ricerche (Comitato Tecnologico).

References

[1] M. Shimura, *J. Electrochem. Soc.* **125** (1978) 190.
[2] A. Di Paola, F. Di Quarto and G. Serravalle, *J. Less Common Met.* **42** (1975) 315 and references therein.
[3] A. Di Paola and F. Di Quarto, *Electrochim. Acta* **22** (1977) 63.
[4] F. Di Quarto, A. Di Paola and C. Sunseri, *J. Electrochem. Soc.* **127** (1980) 1016.
[5] A. Di Paola, F. Di Quarto and C. Sunseri, *Corros. Science* **20** (1980) 1067.
[6] G. A. Korchinskii and G. V. Andreev in 'Novosti Elektrokhim. Org. Soedin. Tezisy Dokl. Elektrokhim. Org. Soedin'. 8th edn (edited by L. G. Feoktistov) Zinatne (1973) pp. 32–3.
[7] E. A. Tomilla, *Ann. Acad. Sci. Fenn.* **1** (1932) 61.
[8] G. M. Yokohama and W. Ishikawa, *Bull. Chem. Soc. Japan* **6** (1931) 275.
[9] O. Glemser and C. Naumann, *Z. Anorg. Chem.* **265** (1951) 288.
[10] O. Glemser, J. Weidelt and F. Freund, *ibid.* **332** (1964) 299.
[11] V. I. Shivonen, *Ann. Acad. Sci. Fenn.* **9** (1921).
[12] M. Farooque and T. Z. Fahidy, *Aiche Simposium Series N. 185* **75** (1979) 128.